

3. Van Cauter, E. & Turek, F. W. in *Endocrinology* Vol. 3 (ed. DeGroot, L. J.) 2487–2548 (Saunders, Philadelphia, 1995).
4. Czeisler, C. A., Weitzman, E. D., Moore-Ede, M. C., Zimmerman, J. C. & Knauer, R. *Science* **210**, 1264–1267 (1980).
5. Späth-Schwalbe, E., Schöller, T., Kern, W., Fehm, H. L. & Born, J. *J. Clin. Endocrinol. Metab.* **75**, 1431–1435 (1992).
6. Mason, J. W. *et al. Psychosom. Med.* **35**, 406–414 (1973).
7. Deinzer, R., Kirschbaum, C., Gesele, C. & Hellhammer, H. *Physiol. Behav.* **61**, 507–511 (1997).
8. Ehrhart-Bornstein, M., Hinson, J. P., Bornstein, S. R., Scherbaum, W. A. & Vinson, G. P. *Endocr. Rev.* **19**, 101–143 (1998).
9. Lavie, P., Oksenberg, A. & Zomer, J. *Percept. Motor Skills* **49**, 447–450 (1979).
10. Follenius, M., Brandenberger, G. & Muzet, A. *Horm. Metab. Res.* **17**, 602–606 (1985).

Air traffic may increase cirrus cloudiness

High-level cirrus clouds can evolve^{1,2} from the condensation trails of aircraft, which form as the mixture of warm, humid exhaust gases and colder, drier air exceeds water saturation³. In addition, the particles in exhaust plumes from aircraft may allow ice nucleation at lower supersaturations than those required under natural conditions⁴. This mechanism is sensitive to environmental conditions, but may occur downstream of the exhaust aerosol source regions. Here I show that cirrus clouds increased in occurrence and coverage in the main air-traffic flight corridors between 1982 and 1991.

I used synoptic cloud reports from land and ship stations for 1982 to 1991 (ref. 5) to establish the relationship between variations in the occurrence of cirrus cloud and the spatial distribution of aviation fuel consumption^{6,7}. During this period there was a large increase in total fuel consumption by air traffic, with an average annual growth rate of 3.2% (ref. 8). I computed the cirrus occurrence frequency at the 3° × 3° resolution from cloud reports (see Supplementary Information). The change in cirrus occurrence frequency is then computed as the difference in frequency between 1987–1991 and 1982–1986, whereas its trend is estimated as the absolute percentage increase along a best-fit line over the 10 years of data.

The average change in cirrus occurrence over land and ocean is plotted against fuel consumption in Fig. 1a, b. Global annual cirrus occurrence increases on average by 1.1% and 3.5% for land and ocean, respectively, with regional average increases of 2.9% to 4.6% over the principal flight corridors (defined as the twenty 3° × 3° grid-boxes with most air traffic). The largest changes correspond to positive trends in cirrus occurrence of 8.5% and 7.0% (Table 1). Over North America, the trend in cirrus occurrence varies between 2.4% and 9.9% per decade, depending on the season. It is largest in December–May, when there is the highest frequency of persistent condensation trails⁹. Between 39° and 42° N, close to

Table 1 Trends in cirrus cloud occurrence, cirrus amount when present and cirrus amount

Land	Occurrence				Annual	AWP	Amount
	DJF	MAM	JJA	SON			
Eurasia	1.2/2.6	-0.8/1.1	1.7/4.4	-0.8/-1.4	0.6/1.6	-1.9/-1.9	0.0/2.9
N. America	7.0/7.8	9.9/16.5	3.2/9.5	2.4/7.3	5.6/13.3		
Ocean	Occurrence				Annual	AWP	Amount
DJF	MAM	JJA	SON				
N. Atlantic	4.5/8.4	5.1/6.3	3.3/8.7	3.9/6.0	4.1/7.1	0.4/-4.2	2.3/1.0
N. Pacific	8.7/5.8	8.4/1.9	5.8/2.5	10.4/4.8	8.4/4.1		

In each column, the first figure reports the trend over the whole region, and the second figure shows the trend over the 20 grid-boxes with most air traffic in 1992. For North America, the second figure is for the 10 grid-boxes with most air traffic. Months (December to November) are denoted by their initial letter; AWP, amount when present. Trends are given as per cent per decade.

the Great Lakes, the trend in annual mean cirrus occurrence is 13.3%, more than twice that for the rest of North America. Over ocean, the trend is also very large in the North Atlantic flight corridor, hence the positive slope in Fig. 1c. Changes in cirrus occurrence over the North Atlantic flight corridor are significantly larger than over the rest of the North Atlantic (Student's *t*-test, *P* = 0.03). Table 1 indicates that, with only one exception, the trend in cirrus increase is larger averaged over the 20 grid-boxes in each region with most air traffic for Eurasia, North America and the North Atlantic Ocean in all seasons.

In the North Pacific Ocean there is the largest increase in cirrus occurrence between 40° and 60° N. There is little air

traffic here, but the region lies downwind of the high-traffic area along the east coast of Asia. It is plausible that cirrus occurrence in the North Pacific is favoured by the presence of soot aerosols emitted by aircraft and transported eastwards to areas where conditions for cirrus formation are often met; a large amount of natural cirrus cloud is found over this region. Along the east coast of Asia there has been a decrease in cirrus occurrence, which might be explained by a decrease in the mean flight level (computed from refs 6,7), which lowers the potential for condensation-trail formation.

A search for other possible causes of increased cirrus, such as the effects of the El Chichón and Mount Pinatubo volcanic aerosols¹⁰, or long-term changes in relative

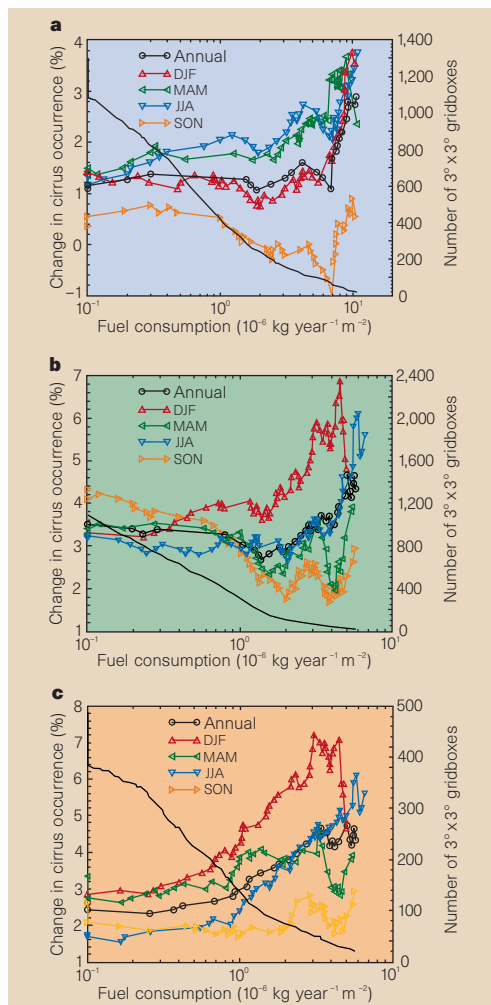


Figure 1 Difference in cirrus occurrence frequency between 1987–1991 and 1982–1986. **a**, Land; **b**, ocean; **c**, North Atlantic Ocean. Results are averaged over grid-boxes with the 1992 fuel consumption at altitudes more than 8 km greater than the values displayed on the x-axis, and show annual means (circles) and seasonal means (triangles). The frequency of cirrus occurrence is defined as the ratio of the number of high-cloud observations to the number of potential high-level cloud observations (situations where low- and middle-level clouds do not completely obscure the higher level of the atmosphere). Only observations meeting the illuminance criterion defined by Hahn *et al.*¹⁵ are included, introducing a bias towards daytime. The bold line represents the number of 3° × 3° grid-boxes from which the annual mean is calculated. The curves are truncated when the number of grid-boxes used to calculate the mean falls below 20.

humidity and climate variations related to the North Atlantic oscillation^{11,12}, showed that none of them, taken individually, is a good explanation for the observed positive trend in cirrus occurrence and its regional distribution.

The trends in cirrus 'amount when present' over the previously defined regions of high fuel consumption are -1.9% and -4.2% for land and ocean, respectively (Table 1). The combination of a large positive trend in cirrus occurrence associated with a negative trend in the cirrus amount when present is consistent with an increasing amount of condensation-trail cirrus covering a small portion of an otherwise clear sky at the cirrus cloud level. This results in a trend in cirrus coverage (cirrus occurrence × cirrus amount when present) of 0.0% averaged over land, rising to 2.9% over the continental regions with most air traffic. Over ocean, these values are 2.3% and 1.0%, respectively, because of the aforementioned contribution of the North Pacific Ocean to the global increase in cirrus occurrence. Both radiative transfer calculations and Earth Radiation Budget Experiment measurements of the net change in radiation associated with high, thin clouds¹³ suggest a 0.2 W m⁻² cloud radiative forcing per 1% of condensation trail or high-level cloudiness. I therefore estimate that the trend in cirrus amount over the continental regions of high air traffic (2.9%, as discussed above) would correspond locally to an additional cloud radiative forcing of about 0.7 W m⁻² between 1982 and 1991. A larger forcing would be expected if calculated from the beginning of commercial jet traffic until the present time. However, we cannot rule out the possibility that the observed change in cirrus amount is not due solely to aviation, or that other climate processes have not masked an even larger aviation impact on cirrus cloudiness. For instance, a previous analysis¹⁴ showed that other regions experienced large positive trends in cirrus amount between 1952 and 1981.

Olivier Boucher

Laboratoire d'Optique Atmosphérique, U.F.R. de Physique, Université de Lille-I, 59655 Villeneuve d'Ascq Cedex, France e-mail: boucher@loa.univ-lille1.fr

1. Seinfeld, J. H. *Nature* **391**, 837-838 (1998).
2. Minnis, P. et al. *Geophys. Res. Lett.* **25**, 1157-1160 (1998).
3. Schumann, U. *Meteorol. Z.* **5**, 4-23 (1996).
4. Jensen, E. J. & Toon, O. B. *Geophys. Res. Lett.* **4**, 249-252 (1997).
5. Hahn, C. J., Warren, S. G. & London, J. *Edited Synoptic Cloud Reports from Ships and Land Stations Over the Globe, 1982-1991, NDP026B* (Carbon Dioxide Information Analysis Center, Oak Ridge National Laboratory, Tennessee, 1996).
6. Baughcum, S. L., Henderson, S. C., Tritz, T. G. & Pickett, D. C. *Scheduled Civil Aircraft Emission Inventories for 1992: Database Development and Analysis* (NASA CR-4700, 1996).
7. Mortlock, A. M. & van Alstyne, R. *Military, Charter, Unreported Domestic Traffic and General Aviation: 1976, 1984, 1992, and 2015 Emission Scenarios* (NASA CR-207639, 1998).
8. *Energy Statistics and Balances of Non-OECD Countries, 1994-1995* 124-125 (International Energy Agency, Organization for Economic Cooperation and Development, Paris, 1997).

9. Minnis, P., Ayers, J. K. & Weaver, S. P. *Surface-Based Observations of Contrail Occurrence Frequency over the U. S., April 1983-April 1994* (NASA Reference Publication 1404, 1997).
10. Jensen, E. J. & Toon, O. B. *Geophys. Res. Lett.* **19**, 1759-1762 (1992).
11. Hurrell, J. W. *Science* **269**, 676-679 (1995).
12. Mächel, H., Kapala, A. & Flohn, H. *Int. J. Climatol.* **18**, 1-22 (1998).
13. Hartmann, D. L., Ockert-Bell, M. E. & Michelsen, M. L. *J. Clim.* **5**, 1281-1304 (1992).
14. Warren, S. G., Hahn, C. J., London, J., Chervin, R. M. & Jenne, R. L. *Global Distribution of Total Cloud Cover and Cloud Type Amounts over the Ocean* (NCAR Technical Note TN-317 + STR, Boulder, Colorado, 1988).
15. Hahn, C. J., Warren, S. G. & London, J. *J. Clim.* **8**, 1429-1446 (1995).

Supplementary information is available on Nature's World-Wide Web site (<http://www.nature.com>) or as paper copy from the London editorial office of Nature.

High metabolic rates in running birds

The ability to increase metabolic rate during locomotion has been important in the structural evolution and evolutionary success of both birds and mammals. Greater endurance capabilities are conferred directly by greater maximal metabolic rates, which vary between species. These maximal rates are known for many mammals¹ but have not been determined for birds. We have measured oxygen consumption in a large flightless bird, the rhea, *Rhea americana*, while it was running on an inclined treadmill, and find an upper limit to aerobic metabolism that is 36 times greater than the minimum resting rate, a factorial increase exceeding that reported for nearly all mammals.

We trained two female rheas (average mass 21.8 kilograms) for two years to run on a treadmill while wearing clear plastic hoods. We then measured linear increases in rates of oxygen uptake while the birds ran up a 16° incline. The maximum rate of oxygen uptake was 2.85 millilitres per kilogram of body mass per second, reached at a running speed of 4.0 metres per second. There were no further increases in oxygen uptake when running speeds were increased to 4.7 metres per second, and plasma lactate concentrations indicated an increasing reliance on anaerobic glycolysis to provide metabolic energy at these higher speeds.

Rates of lactate accumulation (4.4 to 6.8 mM min⁻¹) and peak concentrations (24.8 mM) matched values reported for mammals running at speeds above their aerobic maximum. Remarkably, the aerobic scope

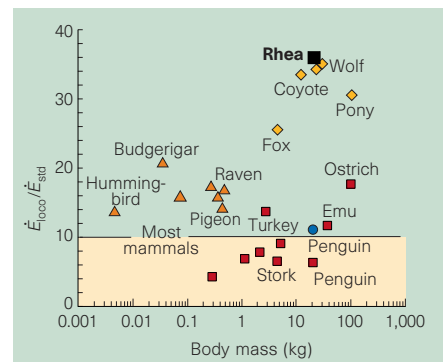


Figure 1 Factorial increases in metabolic rates above resting minimum for rheas and athletic mammals at the aerobic maximum and for other avian species at the highest rates available. Triangles, flying birds; squares, walking and running birds; circles, swimming birds; and diamonds, running mammals.

(the maximum aerobic metabolic rate divided by the minimum resting rate²) of these relatively inactive birds is more than 3.5 times those of typical mammals¹, and equals those of some of the most capable mammalian endurance runners (Fig. 1).

Although the rheas' factorial increase in anaerobic metabolism is 1.7 times greater than the highest previously reported avian values (Fig. 1), we believe that their aerobic scope is representative of birds in general. Previous avian values do not provide evidence of being upper limits; they are probably below species' maxima, but to unknown extents. Nonetheless, the minimum metabolic increase required for flight³ of 15 times the resting value exceeds the aerobic power of a typical mammal by a factor of 1.5, and most avian species can fly. Even birds with more limited endurance, such as the penguin and domestic fowl, can increase their aerobic metabolism by as much as a typical mammal^{4,5}. We suggest that, on average, the aerobic scope of birds exceeds those of mammals by a factor of two or more.

The structural basis of the rheas' aerobic power indicates that respiratory structure-function relationships, previously undetermined for birds, are quantitatively similar to those of mammals throughout most of the respiratory system, and are consistent with the concept of reasonable animal design⁶ (Table 1). Rheas, like aerobic mammals, achieve maximal high rates of oxygen uptake with existing cardiovascular and muscular structures, rather than by

Table 1 Mitochondrial volume densities and capillary densities of rhea muscles

Muscle	Bird A		Bird B	
	V _m (%)	N _c (mm ⁻²)	V _m (%)	N _c (mm ⁻²)
Iliotibialis lateral	10.1	803	6.5	787
Gastrocnemius	11.8	864	7.9	642
Pectoralis	4.2	411	4.2	469
Humerotriceps	4.3	619	4.9	508

Mean mitochondrial volume densities (V_m) and capillary densities (N_c) for leg muscles (iliotibialis and gastrocnemius) were 9.04% and 774 mm⁻², respectively; values for wing muscles (pectoralis and humerotriceps) were 4.37% and 502 mm⁻², respectively, for the rheas. Values for equivalent leg muscles of similarly sized mammals: for a 28-kg dog, V_m = 9.1% and N_c = 884 mm⁻²; for a 26-kg goat, V_m = 3.4% and N_c = 719 mm⁻².